Key Points:
- Holocene mean subsidence rates of 2.6–4.3 mm/a in the Donggi Cona pull-apart basin could be calculated
- Sediment composition and fossil remains indicate pond status in the lake basin during the Late Glacial
- Higher frequency of neotectonic activity can be differentiated from hydroclimatic impact

Author Contributions:
Conceptualization: Dada Yan, Bernd Wünnemann
Formal analysis: Bernd Wünnemann, Yongzhan Zhang
Funding acquisition: Bernd Wünnemann
Project Administration: Dada Yan, Bernd Wünnemann
Validation: Nils Andersen
Visualization: Bernd Wünnemann
Writing – original draft: Dada Yan, Bernd Wünnemann
Writing – review & editing: Dada Yan, Bernd Wünnemann, Yongzhan Zhang, Nils Andersen

Neotectonic Subsidence Along the Cenozoic Kunlun Fault (Tibetan Plateau)

Dada Yan[1,2], Bernd Wünnemann[1,2] , Yongzhan Zhang[3], Kai Hartmann[2], Bernhard Diekmann[4], and Nils Andersen[5]

[1]Faculty of Geosciences and Environmental Engineering, Southwest Jiaotong University, Chengdu, China, [2]Institute of Geographical Science, Freie Universität Berlin, Berlin, Germany, [3]School of Geography and Ocean Science, Nanjing University, Nanjing, China, [4]Alfred Wegener Institute Helmholtz Centre for Polar and Marine Research, Potsdam, Germany, [5]Leibniz Laboratory for Radiometric Dating and Stable Isotope Research, Christian Albrechts Universität zu Kiel, Kiel, Germany

Abstract Many lake basins on the Tibetan Plateau are affected by tectonic activity. It is therefore important to consider seismotectonic influence on lake evolution when discussing climate impact on hydrology and sediment budgets. Lake Donggi Cona serves as an example to demonstrate the influence of the Kunlun left-lateral strike-slip fault on lake formation with subsidence in the pull-apart basin. The results show that comparable fluvial sandy sediments generated at low lake levels during the Late Glacial and early Holocene occur at different water depths within a double lake-internal pull-apart structure, suggesting mean subsidence rates of 2.6–4.3 mm/a since 13.5 cal. ka BP. Such pulses prevailed throughout the Holocene, pointing to repeated seismic events and ongoing neotectonic activity. Sediment distribution and changing morphological shape by subsidence are important factors that affected other lakes on the Tibetan Plateau and enable us to distinguish between neotectonic and paleoclimatic impacts.

Plain Language Summary Lake basins on the Tibetan Plateau are frequently affected by tectonic activity. Lake Donggi Cona basin serves as an example how such activities impact lake evolution throughout the last 13,500 years, apart from hydroclimatic influence. Sediment distribution in the lake basin indicates a shallow basin morphology during the Late Glacial and early Holocene that was successively influenced by subsidence toward a deep central part of the basin. Subsidence rates were calculated to about 2.6–4.3 mm/a, indicating frequent seismotectonic events within the double pull-apart basin at the Kunlun left-lateral slip fault. This basin serves as an example that neotectonic influence has to be considered when discussing hydroclimatic variability over time.

1. Introduction

The Tibetan Plateau represents an area of prominent uplift and associated faulting in the course of the late Cenozoic collision of the Indian subcontinent with Eurasia. Fault zones over the plateau include tectonic basins related to strike-slip movements that often accommodate lake systems in their deeper parts. Sedimentary architectures, subaquatic topography and paleolimnological information may help to decipher both tectonic pulses and climate-related processes that go hand in hand, but are usually hard to unravel. However, studies of lake-catchment interactions on tectonic-related lakes on the Tibetan Plateau have the chance to distinguish between neotectonic and paleoclimatic processes clearly.

Pull-apart basins are associated with two strike-slip basin side wall faults along their long axis and frequently show a rhombic shape with a well-defined length/width ratio of 3 (Aydin & Nur, 1982; ten Brink & Flores, 2012). Detailed studies on such basins in terms of tectonic structure, geometry, and subsidence history refer to the Dead Sea (ten Brink & Flores, 2012), Sea of Marmara (Armijo et al., 2005), Sea of Galilee (Hurwitz et al., 2002), Salton Sea, California (Brothers et al., 2009) or on laboratory modeling of pull-apart development (Wu et al., 2009), for example, while information from pull-apart systems on the Tibetan Plateau is scarce and mainly considered in the context of normal fault extension and strike-slip faults (e.g., Beng Co and Gyaring Co fault zone) in southern/central Tibet (Armijo & Tapponnier, 1986) and along the Haiyuan fault (Gaudemer et al., 1995; Liu-Zeng et al., 2015). The Donggi Cona pull-apart basin is a segment along the Kunlun fault crossing the northern Tibetan Plateau as one of the major left-lateral strike-slip faults that

accommodate Indian-Asian convergence by distinct fault trace, extraordinary length and frequent earthquakes (Guo et al., 2007; Harkins et al., 2010; Lin et al., 2002; Tapponnier et al., 2001). Slip rates of 5.5 ± 0.7, 6.5 and 10.3 mm/a were estimated along the Donggi Cona pull-apart segment in several tectonogeomorphic investigations (Fu et al., 2005; Guo et al., 2007; Van der Woerd et al., 2002). Meanwhile, vertical offsets of 0.4–0.8 m connected with the 1937 earthquake and larger cumulative vertical offsets were reported east of the basin (Van der Woerd et al., 2002) and for the Kusai Hu segment further west (Li et al., 2005). However, vertical offsets within the Donggi Cona pull-apart basin through time remain unknown.

Most of the lake basins on the Tibetan Plateau are located in the endorheic part of the plateau (Armijo & Tapponnier, 1986), but little is known, how these basins and their sedimentary processes developed during the late Quaternary under tectonic impact. Existing seismic profiles from Donggi Cona were discussed only in terms of general basin structure based on bathymetry data and sedimentary composition of cores from the 39 m terrace below the present lake level in light of climatic impact without considering tectonically induced subsidence rates (Dietze et al., 2010; Opitz et al., 2012).

Here we used a new well-dated in-lake sediment core related to the maximum sediment column at the depocenter with high-resolution seismic profiles across western and central Donggi Cona and compared an existing sediment core at shallower site as well as seismic profiles over the eastern lake in order to estimate subsidence rates with reference to water level throughout the last 13,500 years.

2. Study Site

The rhomb-shaped Donggi Cona pull-apart lake (also reported as Dongxi Co or Tuosu Hu, 35.3°N, 98.5°E) occupies the western part of the 155 km long Donggi Cona-Anyemaqen segment, east of Kunlun left-lateral strike-slip fault, that intersects the lake from WNW to ESE with an angle of ca. N110-115°E (Dietze et al., 2010; Fu & Awata, 2007; Van der Woerd et al., 2002).

At an elevation of 4,090 m above sea level, the lake itself has an area of ca. 300 km^2 with a catchment of about 3,000 km^2 and a maximum water depth of 95 m. It is fed by a larger river originating in the push-up structure of the glaciated Anyemaqen Mountains south-east of the lake basin (Van der Woerd et al., 2002) and developed a wide-spread fluvial-alluvial plain at the eastern side that fills a part of the pull-apart basin. Two more important inflows on the northern side of the lake basin originate in the nearby formerly glaciated mountain ranges. The lake has currently an outflow toward the Qaidam Basin on the western side, thus being an open system.

Annual average temperature is estimated to −3.3 °C and precipitation amounts for 332.5 mm/a, according to the meteorological data from the nearest station at Madoi town, some 50 km south (Yan et al., 2020). Discontinuous permafrost is detectable in the entire region.

3. Methods

Acoustic sub-bottom profiling of 16 transects was conducted in 2006 (Dietze et al., 2010) and a new sub-bottom profiling along transect no. 1 (Figure 1) was repeated in 2009 (details in Supporting Information S1) In this study we refer to three seismic transects (Figure 1) from both cruises for further discussion.

In 2016, we obtained a sediment core DCO4 from the deepest part of the lake basin at 90 m water depth by using a UWITEC-90 drilling device. The total length of the spliced core reached 9.48 m sediment depth. The core segments were cut lengthwise and sampled in 1 cm intervals for further analyses, e.g., loss on ignition measurements following Heiri et al. (2001) and grain size analyses in 5 cm intervals by a Malvern Master sizer 2000 (Figure 3b).

Radiocarbon-AMS dating of 17 bulk samples from core DCO4 was performed at Beta Analytics, US (Table S1 in Supporting Information S1). A linear interpolation of the upper 5 ages to the core top yielded an age of 2,679 years as the mean reservoir error and subtracted from all original ^{14}C ages before calibration on the base of the IntCal20 dataset (Reimer et al., 2020). The consistent age model tracing back to 13.75 cal. ka BP was established by Bacon in R (Blaauw & Christen, 2011, Figure 3, Table S1 in Supporting Information S1).
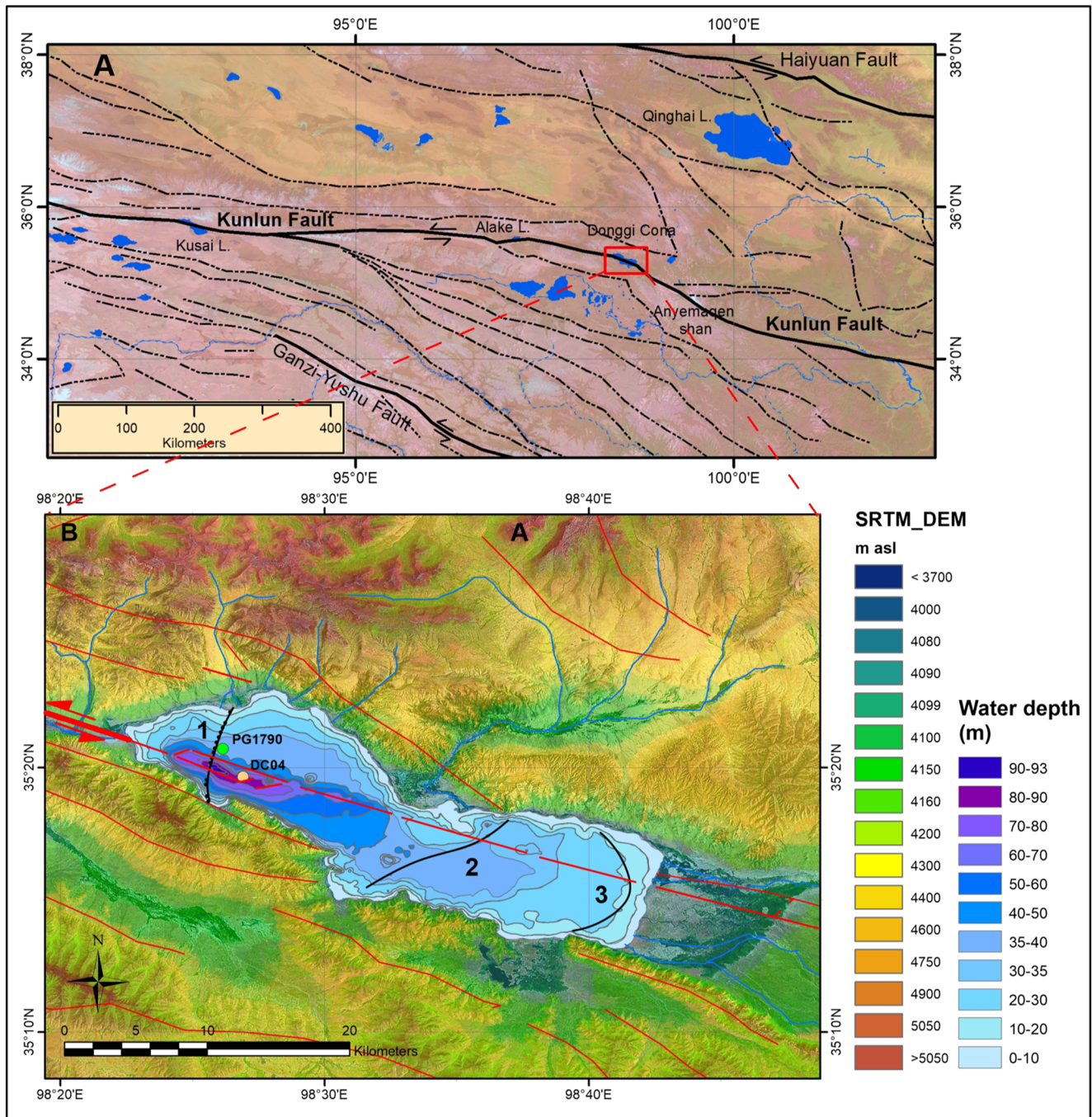
Figure 1. (a) Overview map of the northern Tibetan Plateau with distribution of lakes, major strike-slip faults and further faults (Guo et al., 2019; Van der Woerd et al., 2002) and (b) the Donggi Cona pull-apart basin with the cross-basin fault (red line and estimated fault: dashed line) along the Kunlun fault system (Van der Woerd et al., 2002) including a double pull-apart structure of faults that encircle the deep part. Red lines outside the basin mark faults according to the Geological map 1:1,500,000 of Tibetan Plateau and adjacent areas (CIGMRCGS, 2004). Locations of core sites (green dot: Opitz et al., 2012; Mischke et al., 2010, orange dot: this study) and seismic transects (black lines): 1 and 2 = this study, 3 = Dietze et al. (2010).

Calculation of the maximum mean subsidence rate is based on the difference depth between the terrace T3 level at site PG1790 (34.7 m) water depth and the core site DCO4 at 90 m water depth, revealing an offset of 55.3 m. However, taking the 13.5 cal. ka BP old sediments at both cores (PG1790: 37.7 m; DCO4: 99.2 m) into account, the difference accounts for 61.5 m. A maximum mean subsidence rate therefore would be between 4.6 and 4.1 mm/a, yielding a mean maximum value of 4.3 ± 0.27 mm/a, assuming a similar water
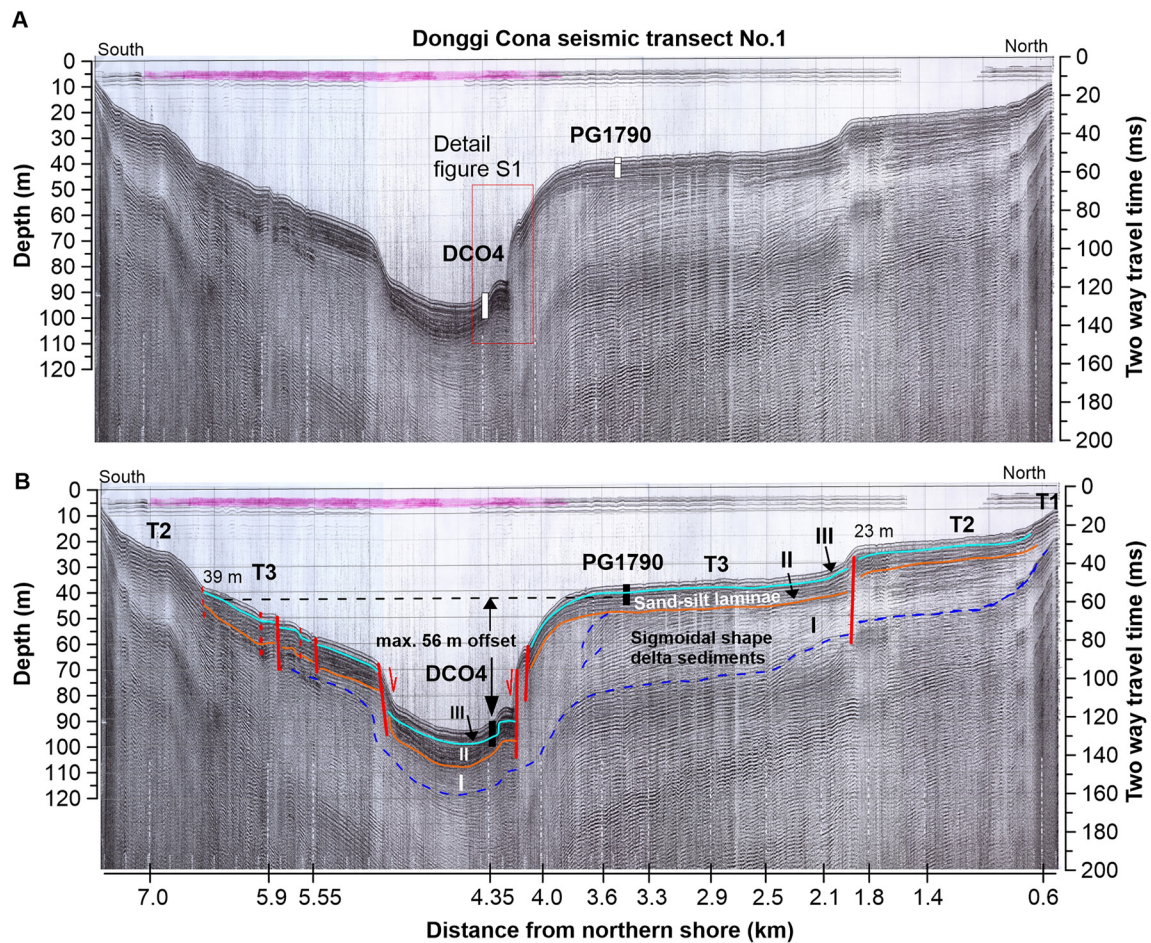
Figure 2. Seismic transect no.1 crossing the graben structure (a) with location of sediment cores PG1790 (Mischke et al., 2010), DCO4 (this study) and identified sedimentary and tectonic structures (B, faults marked in red solid lines. Blue dashed lines remain less obvious). Numbers I–III refer to different sediment types of older than LGM (i), Late Glacial-early Holocene (II) and mid-to-late Holocene age (III), according to the provided chronologies.

depth and thus elevation of the depocenter (core DCO4) with the terrace T3 level at core site PG1790, indicated by the ostracod associations at 13.5 cal. ka BP. A minimum mean subsidence rate of 2.6 mm/a after 8 cal. ka BP was estimated based on the 21 m vertical separation of Unit III by a single fault.

4. Results and Discussions

4.1. Seismic Profiles

The bathymetric profile shows three terraces in the lake with the highest one (T1) at 10 m water depth (Figure 2). The seismic transect crossing the western part of the deep, 6 km long and ca. 2 km wide graben structure (Figure 2), shows the other two distinct terrace levels at 20–23 m (T2) and 33–39 m (T3) water depth on the northern lake bottom side with clearly noticeable faults located along the side walls of the graben (Figure 2 and Figure S1 in Supporting Information S1). They can be noticed by offsets between sedimentary layers. In general, the seismic profile no.1 (Figure 2 and Figure S2 in Supporting Information S1) shows high impedance contrasts with parallel reflections in most parts. They can be divided into three units: unit I comprises lower impedance contrast with a sigmoidal shape of mainly parallel reflections north of the graben but continues with an offset beneath the deep graben and commences along the southern slopes. Unit II has a higher impedance contrast with mainly parallel structures, with a clear unconformity against unit I. Unit III comprises variations between parallel and homogenous lower impedance contrast that can be also assigned to a drape of the former unit.
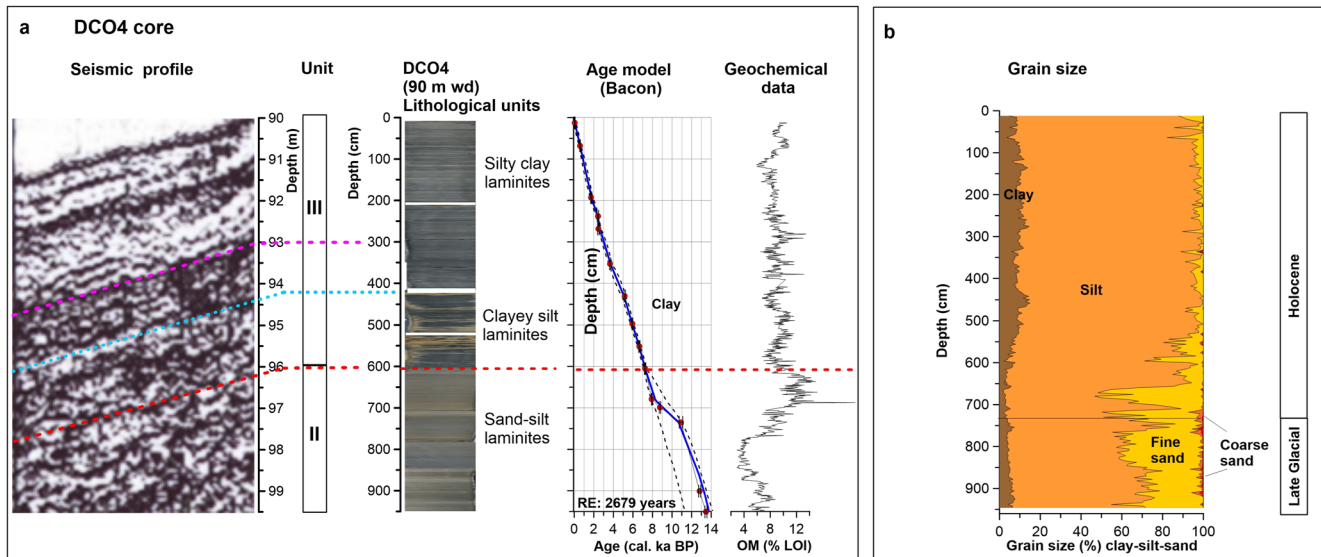
Figure 3. (a) Seismic sequence and sediment stratigraphy of core DCO4 with Bacon age model and organic matter content distribution. The units refer to Late Glacial-early Holocene (II) and the mid-to late Holocene (III) periods; (b) Grain size distribution in core DCO4. Colored dashed lines refer to the boundary of changes in impedance contrast and sediment composition in relation to age, while the red one marked the lower boundary of Unit III.

The convex upward structures of deformation at the northern lake bottom side (Figure 2 and Figure S1 in Supporting Information S1) indicates that young pressure ridges as a common feature of strike-slip faults and ruptures occurred in the lake, although it was only frequently observed in the western catchment during the previous investigations along the Kunlun strike-slip fault outside the lake basin related to the 1937 earthquake (Li & Jia, 1981).

The sediment core PG1790 (34.7 m water depth, Mischke et al., 2010) was located on T3 (39 m water depth), ca. 1 km away from the steeper slope down to the graben bottom. The core DCO4 (90 m water depth) was located ca. 2 km east of the seismic transect and was placed into Figure 2 after comparing the morphology based on bathymetry. The offset between T3 at PG1790 site down to the lake bottom (DCO 4 site) reaches 55.3 m. The minimum vertical offset of 21 m is estimated between the lower Unit III in DCO4 (96 m incl. 6 m-thick sediment) to the upper slope between the pressure ridges (75 m water depth). A vertical offset as low as 10 m in Figure S1 in Supporting Information S1 was not used for calculation because of the potential bias by the young pressue ridge of deformation.

The low-resolution seismic profile no. 2 east of the graben structure shows a clear vertical offset of about 6 m between terrace T3 (here at ca. 32 m depth) and the lake bottom (Figure S3 in Supporting Information S1). Seismic transect no. 3 across the eastern boundary of the lake shows that main river branches in the north and south were likely incised close to the level of T3 terrace by fluvial activity connected to the south-eastern fluvial system from the Anyemaqen Mountains (Figure S4 in Supporting Information S1). It demonstrates subaerial erosive incisions related to a fall in base level during lake low stand (>36 m lower than today), which were refilled during successive reflooding in the lake basin. Considering that the main strike-slip fault occurred south of the northern river channel and continues on land east of the lake basin, and that the mole tracks are also clearly visible with the same direction within the Donggi Cona-Anyemaqen segment (Van der Woerd et al., 2002), tectonic activity can be estimated. However, its influence on the formation of these vertical offsets could be of minor importance compared with the climate-induced low lake level.

4.2. Sediment Compositions

Comparing the seismic profile no.1 with the core DCO4 (Figures 3a and 3b), unit II consists mainly of sandy-silty sediment laminites since 13.5 cal. ka BP until the middle Holocene, in line with the generally lower impedance contrast and very weak parallel seismic reflections. Grain size compositions (Figure 3b) demonstrate high proportions of all sand fractions (up to 45%), while during the early Holocene, after ca.

9 cal. ka BP, higher sand content refers to fine sand only. Unit III represents the upper 6 m of the sediment with variations in impedance contrast and partly weak parallel reflections. They represent mainly fine-grained clay-silt sediments with variable laminae thickness, of which dense laminites correspond with higher impedance contrast, confirmed by grain size analysis (Figure 3b). These sediments comprise the Holocene after ca. 7 cal. ka BP (Figure 3a).

The seismic profile and sediment compositions at PG1790 (T3) site both show consistent features in regard to the depositional environment (Dietze et al., 2010; Figure S2 in Supporting Information S1). Weakly laminated silty sand occurred in the lower part of the core until ca. 18.7 cal. ka BP, followed by sandy-silty laminites until ca. 13.5 cal. ka BP. This composition is consistent with sandy laminites in core DCO4 for the same time period (unit II). Moreover, the robust chronologies for the last 13.5 cal. ka BP as a base for calculating offsets can be inferred from the increase of organic matter and total organic carbon with the onset of climate warming during the early Holocene (Figure 3a and Figure S2 in Supporting Information S1).

4.3. Subsidence in the Lake Basin

Based on the two sediment records from the terrace T3 and the depocenter in the western lake we can calculate subsidence rates since 13.5 cal. ka BP. A pond status at Lake Donggi Cona was suggested during the Late Glacial based on the reanalysis of sediment compositions and ostracod associations in core PG1790 (T3 level, Yan et al., 2020). In addition, the comparable dominances of ostracods *Eucypris mareotica*, *Limnocythere inopinata*, and *Ilyocypris* sp. and their well-preserved shells*,* indicating autochthonous ostracod origin and the same pond situation with slightly flowing water condition at DCO4 site suggest a similar water depth and thus elevation at the two core sites during the period (Yan et al., 2020). Furthermore, the similar laminated sand alternating with fine components in DCO4 supports the very shallow water cover at the lake depocenter as limited distance and variable flow velocities are required for fluvial sandy sediment transportation and deposition, mainly consisting of fluvial sandy sediment sequences. The rather low lake level was also confirmed by the deep incision of the fluvial systems at the eastern side of the lake basin (Figure S4 in Supporting Information S1), that nearly reached the T3 level until a significant change to dominant fine-grained components (silt/clay) since the mid-Holocene could be observed.

In consequence, we can calculate from the difference between the respective sediments in PG1790 at 3 m core depth and 9.2 m core depth in DCO4 a maximum mean subsidence rate of 4.3 ± 0.27 mm/a for the last 13.5 cal. ka BP along the depocenter of the western basin with an uncertainty of about 3 m deviation of the old sediment surface compared to the modern one. Moreover, we calculated a minimum mean subsidence rate based on the vertical offset of the unit III (lower boundary at 96 m) to the steep slope between the convex structures on the northern graben side (75 m, Figure S1 in Supporting Information S1) and revealed a rate of 2.6 mm/a since 8 cal. ka BP. However, sediments in Units II and III were deposited atop the preexisting pull-apart trough with no age control (Figure S1 in Supporting Information S1), thus the true minimum offset of the base of unit III is very difficult to measure. Thus, this calculation even including the other two units suffers from high uncertainty due to the unclear position of the unit I at that time and no age determination for the lower boundaries of the other two units.

Such subsidence rates are reasonable as: (a) laboratory models of pull-apart development show a comparable geometry as observed here at Donggi Cona with significant higher subsidence rates along the depocenters than its marginal zones, indicating a late stage of transtensional pull-apart basin development including a double pull-apart structure across the deeper parts of the lake (Figure 1), supporting a strong subsidence in that part of the basin. A similar development can be observed for an aerial analog at Kusai Lake in the western part of the Kunlun fault (Figure 1a); (b) the existing morphological steps at the normal faults (Doglioni et al., 1998) clearly indicate that the subsidence rate in the western part of Donggi Cona was above the sedimentation rates (0.7 mm/a at DCO4 and 0.25 mm/a at PG1790 sites). Tapponnier et al. (2001) assumed recurrence times of strong earthquakes (M > 7.5) between 400 and 1,000 years, implying at least 12–30 events for the Holocene (12 cal. ka BP) and they mentioned that frequent smaller events took place prior or afterward to a big one with comparable rupture parameters. This can be confirmed by succeeding nearby earth quakes in 1963 (M = 7), 1971 (M = 6.3) (Xiao et al., 1988) and a very strong one along the wider Kunlun fault in 2001 (M = 8.1) (Wen et al., 2009). However, taking the 420 years for earthquakes as a mean re-occurrence interval into account (Van der Woerd et al., 2000) we could expect at least 30–32 events
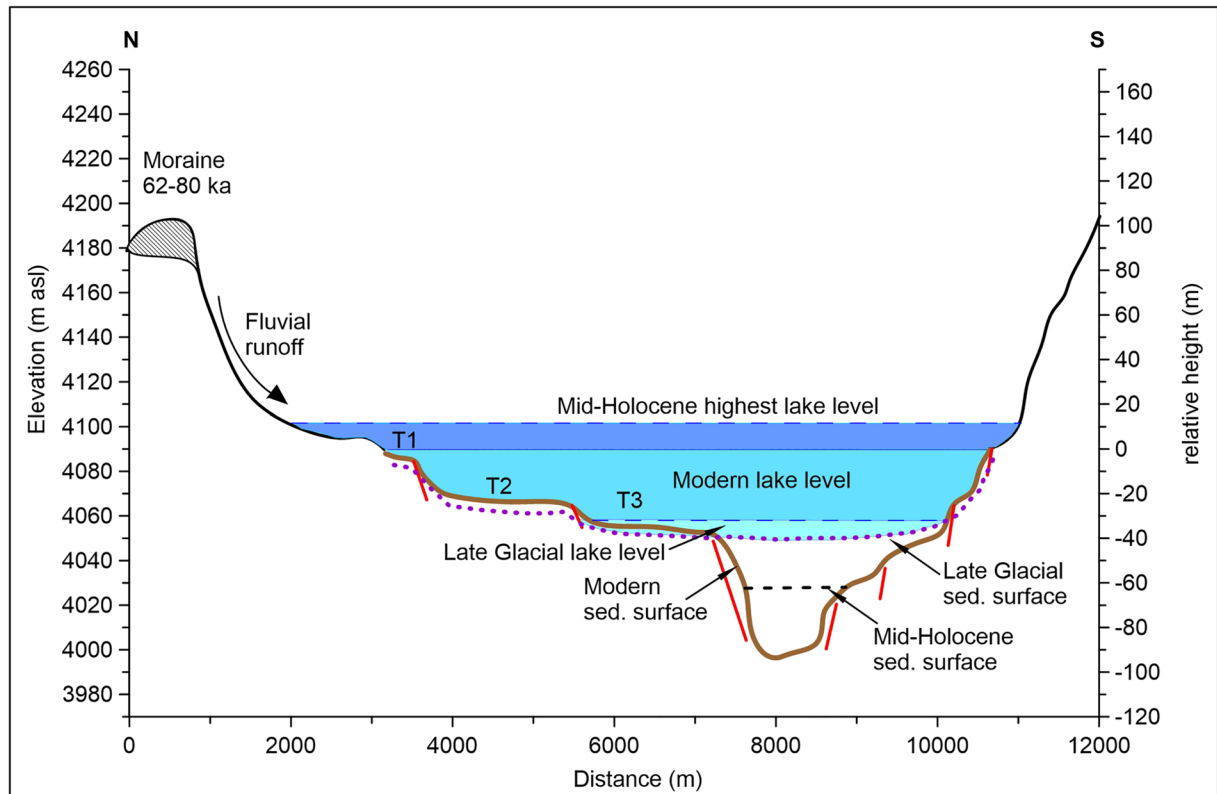
Figure 4. Sketch across the Donggi Cona pull-apart basin with modern, mid-Holocene and Late Glacial basin morphology and lake levels since 13.5 cal. ka BP (after Yan et al., 2020). Red solid lines indicate faults. T1-3 mark submersed terraces, see also Figure S5 in Supporting Information S1.

during the last 13.5 cal. ka BP that evolved as a migrating depocenter in the western part of the lake. A similar earthquake to the 1937 one occurred near Madoi ($M = 7.4$) on May 22, 2021, indicating that the tectonic influence on Donggi Cona could be more frequent than the previous estimations; and (c) comparable subsidence rates were caused by neotectonic activity in the Gaxun Nur basin, north central China (Hartmann et al., 2011), or in the Marmara Sea with development of scarps and up to 6 mm/a offset at the pull-apart margins (Armijo et al., 2005) and even higher subsidence rates in the Salton Sea (Brothers et al., 2009) and in the Dead Sea (ten Brink & Flores, 2012).

The thick sequences of fluvial sands at both Donggi Cona core sites indicate an increased sediment supply accelerated by the subsidence during the late Glacial and early Holocene periods although the climatic conditions were not optimal (Yan et al., 2020). In addition, the observed subaquatic terraces in Donggi Cona may have formed during earlier stages of the pull-apart development and incorporated the result of climate-induced lower lake stages during the Holocene.

Less subsidence is documented in the middle part of the lake with clear offset of ca. 6 m (Figure S3 in Supporting Information S1), which probably formed during shorter time periods within the Holocene as tectonic induced slip rates were calculated based on Holocene ages in the east of Donggi Cona-Anyemaqen segment (Tapponnier et al., 2001). The older observed sediments with sigmoidal shape (unit I) assigned to prior Last Glacial Maximum (ca. 23-20 cal. ka BP) probably correspond to fluvial deposits which were connected with youngest lateral moraines in the northern catchment dated to between 80 and 62 ka (Rother et al., 2017), enhanced by the melting process afterward.

Interesting is that the lake remained very shallow during the Late Glacial and the early Holocene despite climate warming and experienced a closed basin for this time period (Figure 4; Opitz et al., 2012). After around 7.5 cal. ka BP the sediments changed to very fine components without significant contribution of fine sand. These sediments commonly draped older sediments, independent of dramatic changes related to basin morphology with some evidence of vertical offsets (Figure 2) and a strong offset at the northern

boundary of the depocenter. We infer that with the onset of the mid-Holocene the lake level increased toward a highest lake stand possibly supplemented by summer monsoon rainfall (Yan et al., 2020, Figure 4 and Figure S5 in Supporting Information S1) that fostered the hydrological change toward an open system possibly by backward erosion at the modern outflow with ongoing subsidence that strongly increased deposition rate and related sediment budget at the center. Such process also provides a chance that increased water volume by postglacial transgression induced overload in the basin to trigger progressive subsidence. This is an ideal example to show that tectonically affected lakes may lead to a more consistent interpretation of lake evolution and morphological shape if tectonic influence is considered.

Comparable processes may apply to lake basins along the Kunlun fault, such as Kusai Lake and Alake lake (Figure 1a) but likely also to lakes along other fault systems over the plateau as long as they are or were connected with active faults that influenced the basin structure and the hydroclimatic evolution of the lakes. However, these seismotectonic influences such as subsidence within a pull-apart basin on the location of depocenters, as seen in the Donggi Cona pull-apart basin were very seldom monitored in paleoclimatic records in the past. The study can be a key to unravel, how to differentiate between tectonic and climatic signals in lake systems, notably the influence on basin morphology and sedimentary conditions. If tectonic influence at Donggi Cona was not considered, an overestimation of the hydroclimatic influence on the lake basin and the region could be the result. The same applies to many other lakes especially on the Tibetan Plateau. It provides a better insight into spatiotemporal processes of neotectonic impact and deepens the results of investigated onshore sites, to separate the progressive changes of the morphological shape influence on the sediment depth increase in a lake basin from climatic aspects when reconstructing hydroclimatic changes.

5. Conclusion

Seismic profiles and sediment records from two sites in Donggi Cona Lake indicate strong subsidence during the Late Glacial and Holocene periods in combination with left-lateral strike-slip movement of the Kunlun fault. Very young pressure ridge in lake was also visible. Similar sediment composition and autochthonous fossil associations in two sediment cores allowed identifying the water depth/lake bottom elevation of the central graben structure which was similar to the elevation of terrace T3 and likely enhanced subsidence after 13.5 cal. ka BP with lake level increase. The increase in water volume and sediment load by postglacial transgression enhanced subsidence as well. It presents an example of the problems when tectonics overprint climatic signals and indicates earthquake events in higher frequency than expected. The importance of seismotectonic events on lake basins on the Tibetan Plateau remains less considered in paleoclimatic reconstructions but may lead to a reinterpretation of sedimentary records and is helpful to understand regional tectonics.

Conflict of Interest

The authors declare no conflicts of interest relevant to this study.

Data Availability Statement

All data are available in the Mendeley Database under https://doi.org/10.17632/5839k8vdzx.1.

References

Armijo, R., Pondard, N., Meyer, B., Ucarkus, G., de Lépinay, B. M., Malavieille, J., et al. (2005). Submarine fault scarps in the Sea of Marmara pull-apart (North Anatolian Fault): Implications for seismic hazard in Istanbul. *Geochemistry, Geophysics, Geosystems*, *6*(6). https://doi.org/10.1029/2004GC000896

Armijo, R., Tapponnier, P., Mercier, J. L., & Han, T.-L. (1986). Quaternary Extension in southern Tibet: Field observations and tectonic implications. *Journal of Geophysical Research*, *91*(B14), 13803–13872. https://doi.org/10.1029/JB091iB14p13803

Aydin, A., & Nur, A. (1982). Evolution of pull-apart basins and their scale independence. *Tectonics*, *1*(1), 91–105. https://doi.org/10.1029/TC001i001p00091

Blaauw, M., & Christen, J. A. (2011). Flexible paleoclimate age-depth models using an autoregressive gamma process. *Bayesian Analysis*, *6*, 457–474. https://doi.org/10.1214/ba/1339616472

Brothers, D. S., Driscoll, N. W., Kent, G. M., Harding, A. J., Babcock, J. M., & Baskin, R. L. (2009). Tectonic evolution of the Salton Sea inferred from seismic reflection data. *Nature Geoscience*, *2*, 581–584. https://doi.org/10.1038/ngeo590

Chengdu Institute of Geology and Mineral Resources, China Geological Survey CIGMRCGS. (2004). *Geological map of the TP and adjacent areas*. ISBN: 7-80544-8663.

Dietze, E., Diekmann, B., Wünnemann, B., Aichner, B., Hartmann, K., Herzschuh, U., et al. (2010). Basin morphology and seismic stratigraphy of Lake Donggi Cona, north-eastern Tibetan Plateau, China. *Quaternary International*, *218*, 131–142. https://doi.org/10.1016/j.quaint.2009.11.035

Doglioni, C., D'Agostino, N., & Mariotti, G. (1998). Normal faulting vs regional subsidence and sedimentation rate. *Marine and Petroleum Geology*, *15*, 737–750. https://doi.org/10.1016/s0264-8172(98)00052-x

Fu, B., & Awata, Y. (2007). Displacement and timing of left-lateral faulting in the Kunlun Fault Zone, northern Tibet, inferred from geologic and geomorphic features. *Journal of Asian Earth Sciences*, *29*, 253–265. https://doi.org/10.1016/j.jseaes.2006.03.004

Fu, B., Awata, Y., Du, J., & He, W. (2005). Late Quaternary systematic stream offsets caused by repeated large seismic events along the Kunlun fault, northern Tibet. *Geomorphology*, *71*, 278–292. https://doi.org/10.1016/j.geomorph.2005.03.001

Gaudemer, Y., Tapponnier, P., Meyer, B., Peltzer, G., Guo, S. M., Chen, Z. T., et al. (1995). Partitioning of crustal slip between linked, active faults in the eastern Qilian Shan, and evidence for a major seismic gap, the 'Tianzhu gap', on the western Haiyuan Fault, Gansu (China). *Geophysical Journal International*, *120*, 599–645. https://doi.org/10.1111/j.1365-246x.1995.tb01842.x

Guo, J., Lin, A., Sun, G., & Zheng, J. (2007). Surface ruptures associated with the 1937 *M* 7.5 Tuosuo Lake and the 1963 M 7.0 Alake Lake earthquakes and the paleoseismicity along the Tuosuo Lake segment of the Kunlun Fault, Northern Tibet. *Bulletin of the Seismological Society of America*, *97*(2), 474–496. https://doi.org/10.1785/0120050103

Guo, P., Han, Z., Mao, Z., Xie, Z., Dong, S., Gao, F., & Gai, H. (2019). Paleoearthquakes and Rupture Behavior of the Lenglongling Fault: Implications for Seismic Hazards of the Northeastern Margin of the Tibetan Plateau. *Journal of Geophysical Research: Solid Earth*, *124*, 1520–1543. https://doi.org/10.1029/2018JB016586

Harkins, N., Kirby, E., Shi, X., Wang, E., Burbank, D., & Chun, F. (2010). Millennial slip rates along the eastern Kunlun fault: Implications for the dynamics of intracontinental deformation in Asia. *Lithosphere*, *2*(4), 247–266.

Hartmann, K., Wünnemann, B., Hoelz, S., Kraetschell, A., & Zhang, H. (2011). Neotectonic constraints on the Gaxun Nur inland basin in north–central China, derived from remote sensing, geomorphology and geophysical analyses. In R. Gloaguen & L. Ratschbacher (Eds.), *Growth and collapse of the Tibetan plateau* (Vol. 353, pp. 221–233). Geological Society, London, Special Publication.

Heiri, O., Lotter, A. F., & Lemcke, G. (2001). Loss on ignition as a method for estimating organic and carbonate content in sediments: Reproducibility and comparability of results. *Journal of Paleolimnology*, *25*, 101–110.

Hurwitz, S., Garfunkel, Z., Ben-Gai, Y., Reznikov, M., Rotstein, Y., & Gvirtzman, H. (2002). The tectonic framework of a complex pull-apart basin: Seismic reflection observations in the Sea og Galilee, Dead Sea transform. *Tectonophysics*, *359*, 289–306.

Li, H., Van der Woerd, J., Tapponnier, P., Klinger, Y., Qi, X., Yang, J., & Zhu, Y. (2005). Slip rate on the Kunlun fault at Hongshui Gou, and recurrence time of great events comparable to the 14/11/2001, Mw ~7.9 Kokoxili earthquake. *Earth and Planetary Science Letters*, *237*, 285–299.

Li, L., & Jia, Y. (1981). Characteristics of deformation band of the 1937 Tuosuohu earthquake (M=7.5) in Qinghai. *Northwestern Seismological Journal*, *3*(3), 61–65. (in Chinese with English abstract).

Lin, A., Fu, B., Guo, J., Zeng, Q., Dang, G., He, W., & Zhao, Y. (2002). Co-seismic strike-slip and rupture length produced by the Ms 8.1 Central Kunlun earthquake. *Science*, *296*, 2015–2017.

Liu-Zeng, J., Shao, Y., Klinger, Y., Xie, K., Yuan, D., & Lei, Z. (2015). Variability in magnitude of paleoearthquakes revealed by trenching and historical records, along the Haiyuan Fault, China. *Journal of Geophysical Research: Solid Earth*, *120*, 8304–8333. https://doi.org/10.1002/2015JB012163

Mischke, S., Bößneck, U., Diekmann, B., Herzschuh, U., Jin, H., Kramer, A., et al. (2010). Quantitative relationship between water-depth and sub-fossil ostracod assemblages in Lake Donggi Cona, Qinghai Province, China. *Journal of Paleolimnology*, *43*, 589–609.

Opitz, S., Wünnemann, B., Aichner, B., Dietze, E., Hartmann, K., Herzschuh, U., et al. (2012). Late Glacial and Holocene development of Lake Donggi Cona, north-eastern Tibetan Plateau, inferred from sedimentological analysis. *Palaeogeography Palaeoecology Palaeoclimatology*, *337–338*, 159–176.

Reimer, P. J., Austin, W. E. N., Bard, E., Bayliss, A., Blackwell, P. G., Bronk Ramsey, C., et al. (2020). The IntCal20 Northern Hemisphere Radiocarbon Age Calibration Curve (0–55 cal kBP). *Radiocarbon*, *62*(4), 725–757.

Rother, H., Stauch, G., Loibl, D., Lehmkuhl, F., Stewart, P. H., & Freeman, T. (2017). Late Pleistocene glaciations at Lake Donggi Cona, eastern Kunlun Shan (NE Tibet): Early maxima and a diminishing trend of glaciation during the last glacial cycle. *Boreas*, *466*, 503–524.

Tapponnier, P., Ryerson, F. J., Van der Woerd, J., Mériaux, A. S., & Lasserre, C. (2001). Long-term slip rates and characteristic slip: Keys to active fault behaviour and earthquake hazard. *Earth and Planetary Science*, *333*, 483–494.

ten Brink, U. S., & Flores, C. H. (2012). Geometry and subsidence history of the Dead Sea basin: A case for fluid-induced mid-crustal shear zone? *Journal of Geophysical Research*, *117*, B01406. https://doi.org/10.1029/2011JB008711

Van der Woerd, J., Ryerson, F. J., Tapponnier, P., Meriaux, A. S., Gaudemer, Y., Meyer, B., et al. (2000). Uniform sliprate along the Kunlun Fault, implications for seismic behaviour and large-scale tectonics. *Geophysical Research Letters*, *27*, 2353–2356. https://doi.org/10.1029/1999GL011292

Van der Woerd, J., Tapponnier, P., Ryerson, F. J., Meriaux, A.-S., Meyer, B., Gaudemer, Y., et al. (2002). Uniform postglacial sliprate along the central 600 km of the Kunlun Fault (Tibet), from ^{26}Al, ^{10}Be, and ^{14}C dating of riser offsets, and climatic origin of the regional morphology. *Geophysical Journal International*, *148*, 356–388.

Wen, Y., Ma, K., Song, T., & Mooney, WD. (2009). Validation of the rupture properties of the 2001 Kunlun, China (M = 8.1), earthquake from seismological and geological observations. *Geophysical Journal International*, *177*, 555–570.

Wu, J. E., McClay, K., Whitehouse, P., & Dooley, T. (2009). 4D analogue modelling of transtensional pull-apart basins. *Marine and Petroleum Geology*, *26*, 1608–1623.

Xiao, Z., Liu, G., Wang, H., & Xie, X. (1988). A preliminary study on the seismic deformation zone at Huashixia in Qinghai Province. *Earthquake Research in China*, *4*(1), 68–74. (in Chinese with English abstract).

Yan, D., Wünnemann, B., & Zhang, Y. (2020). Late Quaternary lacustrine Ostracoda and their implications for hydro-climatic variation on Northeastern Tibetan Plateau. *Earth-Science Reviews*, *207*, 10325.